**Article:**
Zhang, Y., Sajjad, M.T., Blaszczyk, O. et al. (2019) Large crystalline domains and an enhanced exciton diffusion length enable efficient organic solar cells. Chemistry of Materials, 31 (17). pp. 6548-6557. ISSN: 0897-4756

https://doi.org/10.1021/acs.chemmater.8b05293

# Large crystalline domains and enhanced exciton diffusion length enable efficient organic solar cells

Yiwei Zhang[1†], Muhammad T. Sajjad[1†], Oskar Blaszczyk[1], Andrew J. Parnell[2], Arvydas Ruseckas[1] and Ifor D. W. Samuel[1]*

1.Organic Semiconductor Centre, SUPA, School of Physics and Astronomy, University of St Andrews, St Andrews, KY16 9SS, UK

2. Department of Physics and Astronomy, University of Sheffield, Sheffield, S3 7RH, UK

Abstract: We studied crystallinity and exciton harvesting in bulk heterojunctions of a semiconducting polymer PffBT4T-2OD and electron acceptor $PC_{71}BM$ which are used to make highly efficient organic solar cells. Grazing incidence wide-angle X-ray scattering (GIWAXS) shows that the size of crystalline domains of PffBT4T-2OD increases to ~18 nm in photovoltaic blends upon thermal annealing at 100 °C for 5 minutes. These domains are larger than the typical exciton diffusion lengths in conjugated polymers. Time-resolved fluorescence measurements show that exciton diffusion length in PffBT4T-2OD increases from ~14 to ~24 nm upon thermal annealing, which enables efficient charge generation in blends with large domains. Solar cells prepared using thermally annealed blends show higher photocurrent, open circuit voltage and fill factor compared to as spin-coated blends which indicates reduced recombination losses. Our results demonstrate advantages of large crystalline domains in organic photovoltaics, providing exciton diffusion is sufficient.

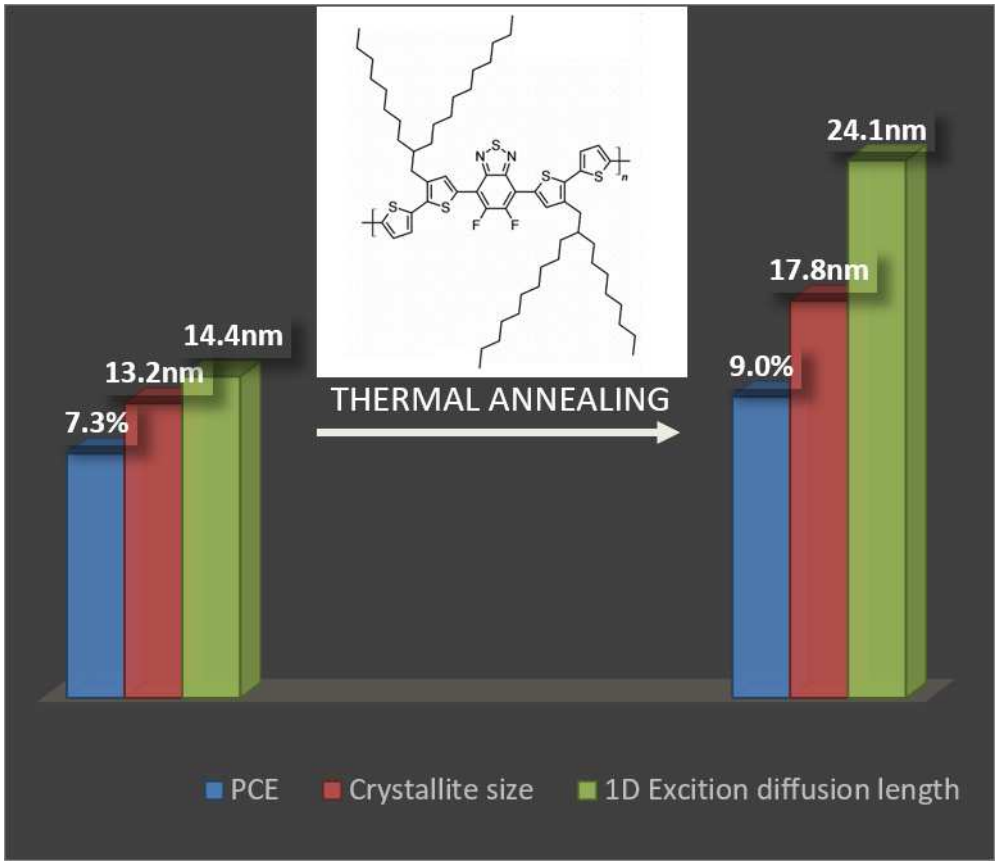


Keywords: organic photovoltaic, thermal annealing, exciton diffusion length, conjugated polymer, fullerene, charge generation

## 1. Introduction

Organic photovoltaics (OPVs) offer many attractive features such as simple fabrication of lightweight thin film solar cells which can be deposited on flexible substrates, low cost and short energy payback time.[1-2] The past decade witnessed rapid development of OPVs, leading to single bulk heterojunction (BHJ) OPV devices with power conversion efficiencies (PCE) of over 12% - a value which is considered sufficient for commercialization.[3-6] However, improvements in OPV to reach 20% should be achievable [7]. To achieve higher PCE, efforts should be made in two directions.[8] Firstly, new organic semiconducting donor and acceptor materials with more favourable energy levels need to be designed and synthesized; secondly, film fabrication and post-deposition treatment methods should be optimized to rationally control the nanoscale morphology of the bulk heterojunction. Primary excitations in OPVs are bound singlet excitons which need to dissociate into free charges in order to contribute to photocurrent.[9-10] The exciton dissociation can either realised via Förster resonance-energy transfer (FRET) or diffusion to a donor/acceptor interface. [11-14] The exciton diffusion length ($L_D$), defined as the distance excitons can travel within their lifetime, is a key parameter in OPV devices as it largely determines the generation of charges from excitons and thus the short circuit current and device efficiency.[15] Because the exciton diffusion length in organic semiconductors is short (typically ~10 nm), a high extent of mixing between donor and acceptor materials is desirable to obtain efficient charge separation. However, after dissociation, free charge carriers need to be extracted to the electrodes to generate current. Large donor and acceptor domains would be best for this as they reduce the interface area and associated recombination losses. Hence there is a trade-off between the desired domain size for charge generation and the size desired for charge extraction. Increasing exciton diffusion length can help to solve this problem by enabling efficient exciton harvesting from larger domains.

The exciton diffusion length of organic semiconducting materials has been measured using different techniques, including volume quenching, [16] surface quenching,[17] exciton-exciton annihilation,[18-19] spectrally resolved photoluminescence quenching,[20] and photo voltage measurements.[21] A lot of effort has been made to enhance the exciton diffusion length by, for example, post deposition treatments such as thermal annealing, solvent vapor annealing and light soaking. Out of these, thermal annealing and solvent vapor annealing are simple, widely used and cost-efficient strategies which allow modification of the crystallinity

of the film in a controllable fashion. We have previously shown that thermal annealing and solvent vapour annealing are effective to improve the exciton diffusion for some organic donor materials. [22-23]

Recently, a highly efficient donor polymer Poly[(5,6-difluoro-2,1,3-benzothiadiazol-4,7-diyl)- alt-(3,3'''-di(2-octyldodecyl) -2,2' ;5', 2'';5'',2''' -quaterthiophen-5,5'''-diyl)], henceforth named as PffBT4T-2OD (chemical structure is shown in **Figure 1(a)**), has been designed and synthesized; single BHJ OPV devices using it as the donor material have achieved PCE of over 11%.[24] The processing parameters have been shown to be crucial in determining the aggregation behaviour of this polymer. [25] The structural analysis by small angle neutron scattering (SANS) showed that thermal annealing at 100 °C for 5 minutes results in coarsening of domains within the PffBT4T-2OD:$PC_{71}BM$ bulk heterojunction films from ~9 to ~13 nm, and that the OPV device efficiency was improved by 20% (from 7.6% to 8.9%). [26]

The aim of the present work is to understand how thermal annealing increases the efficiency of these solar cell devices. By combining the complementary techniques of GIWAXS, time-resolved spectroscopy and space charge limited current (SCLC), we investigated the effect of thermal annealing on domain size, exciton diffusion length and charge mobility. We find that upon thermal annealing, the crystallite size increases from ~13 to ~18 nm, exciton diffusion coefficient from $0.9 \times 10^{-3}$ to $2.7 \times 10^{-3}$ $cm^2/s$ and a corresponding 1-dimensional exciton diffusion length from 14.4 to 24.1 nm. Large crystallite size is beneficial for better charge extraction and long exciton diffusion length helps to realize the highly efficient exciton dissociation. The combined effect of both larger crystallite domain size and longer exciton diffusion length leads to an enhancement of more than 20% in device efficiency. This work differs from our previous work on small molecules where we used solvent vapour annealing to enhance the exciton diffusion and device performance.[27] In the present work we use a more efficient donor polymer with the main focus on the widely used technique of thermal annealing and the use of X-ray to explore the structural changes occurring.

## 2. Experimental methods

### *2.1 Materials and film fabrication*

The semiconducting polymer PffBT4T-2OD was purchased from California Organic Semiconductors Inc, and dissolved in a solvent mixture of chlorobenzene (CB): o-dichlorobenzene (oDCB): 1,8-Diiodooctane (DIO) (volume ratio 48.5: 48.5: 3) and stirred at 90°C overnight before spin coating. Solutions with polymer concentrations ranging from 3 to 14 mg/ml were spin-coated at 1000 rpm to form thin films of thicknesses ranging between 45 and 300 nm; the film thickness was determined by spectroscopic ellipsometry. To investigate the effect of thermal annealing, for all the experiments two sets of samples were prepared: one set was thermally annealed at 100 °C for 5 minutes and another set was without post deposition treatments for comparison purposes. The processing of PffBT4T-2OD films was conducted in a nitrogen-filled glove box. For GIWAXS experiments and device fabrication, $SiO_2$ and glass with pre-patterned ITO substrates were used respectively; for exciton diffusion measurements, films were spin coated on fused silica substrates. All the substrates were ultrasonic cleaned in acetone, isopropanol and deionized water sequentially, each for 5 minutes; followed by oxygen plasma treatment for 3 minutes before use.

### *2.2 Absorption and steady state PL*

Steady absorbance was determined using a Cary 300 UV-visible spectrophotometer; steady photoluminescence spectrum was recorded using an Edinburgh Instrument FLS980 Spectrometer; an excitation wavelength of 515 nm was used.

### *2.3 OPV device fabrication*

For OPV device fabrication, the conventional structure of ITO/PEDOT:PSS/active layer/Ca/Al was used (as shown in **Figure 1(c)**). PEDOT:PSS (Clevios Al 4083) was spin coated onto the pre-cleaned substrates and then annealed at 120ºC for 10 minutes in air before being transferred to the glove box. Then the blend of PffBT4T-2OD:$PC_{71}BM$ (weight ratio of 1:1.2) was spin coated from the solution of the above-mentioned solvent mixture with a total concentration of 20 mg/ml. After drying for 3 hours in glove box and a further 30 minutes in a vacuum chamber, one set of the films were annealed at 100 °C for 5 minutes. Then the electrodes, consisting of calcium (5 nm) and aluminium (100 nm) were evaporated in a thermal evaporator under a vacuum of $\sim 10^{-6}$ mbar. Finally the devices were encapsulated using UV-cured epoxy and a glass slice (cover slip ?).

The photovoltaic properties were characterized by a Sciencetech solar simulator and a Keithley 2400. The irradiance level was calibrated by a silicon detector and a KG-5 filter. The

devices were exposed to AM1.5 solar spectrum with an irradiance level of 100 mW/cm$^2$ during J-V characterization. The external quantum efficiency (EQE) was measured by exposing the device to monochromatic light supplied from a Xenon arc lamp and a monochromator.

### *2.4 Grazing-Incidence Wide-Angle X-ray Scattering (***GIWAXS***)*

GIWAXS measurements were performed using a Xeuss 2.0 SAXS/WAXS laboratory beamline using a liquid Gallium MetalJet (Excillum) X-ray source (9.2 keV, 1.34Å); scattered X-rays were detected by a Pilatus3R 1M detector.

### *2.5 Surface quenching of fluorescence*

For the fluorescence surface quenching measurements, a cross-linked fullerene derivative [6,6]-phenyl-C61-butyric acid styryl dendron ester (PCBSD) is used to perform as a fluorescence quencher. To prepare the quencher layer, PCBSD was dissolved in dichlorobenzene solution and stirred at 75 °C for at least 5 hours. The solution was filtered through a 0.1 μm PTFE filter before being spin coated onto a fused silica substrate. The resultant films were then annealed at 170 °C for 40 min to facilitate cross-linking and spinning washed by chlorobenzene to remove any un-crosslinked residual material. All the processing of cross-linked PCBSD was also conducted in a nitrogen-filled glove box. The PffBT4T-2OD films were fabricated on top of fused silica and cross-linked PCBSD respectively. Different solution concentrations were selected to realize three sets of films with different thicknesses. Time resolved fluorescence decay measurements were conducted under vacuum. The samples were excited by 200 fs light pulses at 515 nm and the time-resolved fluorescence was recorded using a Hamamatsu C6860 streak camera. Here it is worth to note that due to the processing parameters are crucial to influence the aggregation properties of PffBT4T-2OD, we did not change the thickness of PffBT4T-2OD to a large extent.

### *2.6 Exciton–exciton annihilation*

For exciton–exciton annihilation, PffBT4T-2OD films were spin-coated on fused silica substrates; the as spin-coated and thermally annealed films were excited by 200 fs laser pulses at 650 nm with a 5 kHz repetition rate with a pulse energy ranging from 2 to 30 nJ and illuminated by a beam of area 0.030 mm$^2$. The pulses were generated using an optical parametric amplifier (OPA) pumped by a Pharos regenerative amplifier (RA) from Light

Conversion Ltd. Time-resolved fluorescence was recorded using a Hamamatsu C6860 streak camera. We also measured the natural fluorescence decay in the absence of annihilation, where pulses of lower energy (oscillator powered laser with 515 nm wavelength and 80MHz repetition rate) was used as exciting light.

## 3.Results

### *3.1 Absorption and photoluminescence spectra*

The absorption spectra of neat PffBT4T-2OD films before and after thermal annealing are shown in **Figure 1 (b)**. The absorption peaks at 689 nm and 627 nm can be attributed to 0-0 and 0-1 vibronic transitions respectively. The main change is a ~10% increase in the absorption coefficient in the spectral range of 570-710 nm upon thermal annealing which suggests more conjugated polymer chains lie in the plane of the film. The photoluminescence (PL) spectrum of the thermally annealed film shows a slightly stronger peak at ~800 nm which is consistent with stronger absorption in thermally annealed films.

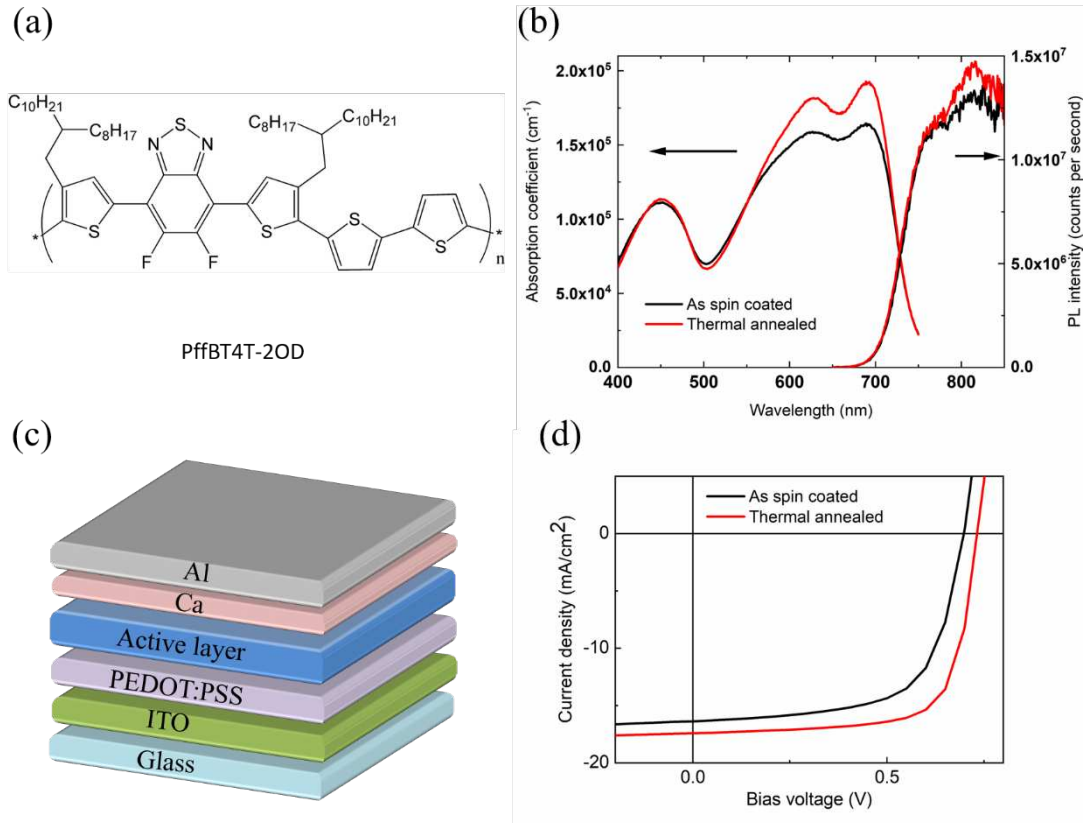

Figure 1. (a) Chemical structure of PffBT4T-2OD (b) absorption coefficient and steady state photoluminescence spectra of as spin-coated and thermally annealed PffBT4T-2OD films. For PL measurement, films were excited at 515 nm. (c) device structure and (d) J-V curves of PffBT4T-2OD:$PC_{71}BM$ bulk heterojunction OPV devices with/without thermal annealing.

### *3.2 OPV device performance*

We fabricated and characterized OPV devices with and without thermal annealing treatment of the active layer. The results of the best and average of 12 devices are presented in **Figure 1 (d)** and **Table 1**. The short circuit current density ($J_{sc}$) was higher in the devices prepared with a thermally annealed blend (17.3 mA/cm$^2$ compared to 16.3 mA/cm$^2$ for as spin-coated device). The results also confirmed by EQE measurements as shown in Figure S1. We also observed that $V_{oc}$ and FF are higher in thermally annealed devices. The overall device efficiency was enhanced from 7.3% to 9.0% by thermal annealing.

Table 1. Device metrics with and without thermal annealing.

| Device type | PCE (%) | $V_{oc}$ (V) | FF (%) | $J_{sc}$ (mA/cm$^2$) |
|---|---|---|---|---|
| Neat | 7.4<br>(7.3 ± 0.14) * | 0.70<br>(0.70 ± 0.00) | 65.1<br>(63.9 ± 1.0) | 16.4<br>(16.3 ± 0.12) |
| Thermally annealed | 9.2<br>(9.0 ± 0.19) | 0.75<br>(0.74 ± 0.01) | 72.4<br>(70.1 ± 1.5) | 17.5<br>(17.3 ± 0.10) |

*The value in the brackets are the average and standard deviation of 12 devices.

### *3.3 Thermal annealing induced crystallite size growth*

To understand the reason behind the improved device efficiency we investigated the crystallinity of PffBT4T-2OD:$PC_{71}BM$ BHJ films using GIWAXS and the results are shown in **Figure 2**. The Bragg peaks at q = 0.30 Å$^{-1}$ and q = 0.59 Å$^{-1}$ were identified as the (100) and (200) crystalline planes defined by stacking of the alkyl chains. The peak at q = 1.79 Å$^{-1}$

corresponds to the π- π stacking distance of the polymer. These peaks become narrower upon thermal annealing which qualitatively suggests an increase to larger crystallites of PffBT4T-2OD.

The crystallite size of PfffBT4T-2OD can be obtained from the full width at half maximum (FWHM) of the (100) peak in the GIWAXS spectra using the Scherrer equation:

$$D = \frac{K\lambda}{\beta \cos\theta} \qquad (1)$$

Here $K$ is the dimensionless shape factor, which is 0.94 in our case; $\lambda$ = 0.134 nm is the X-ray wavelength used in the measurements; $\beta$ is the FWHM of the peak (in radians) and $\theta$ is the Bragg angle. We found that the crystallite size of PffBT4T-2OD in the blends increases from 13.2 to 17.7 nm upon thermal annealing (see **Table 2**). We also measured the crystallite size of neat films of PffBT4T-2OD and observed enhancement from 8.8 to 15.1 nm. Our results are consistent with previous reports where the coarsening of PffBT4T-2OD domains in the bend with $PC_{71}BM$ was observed.[26]

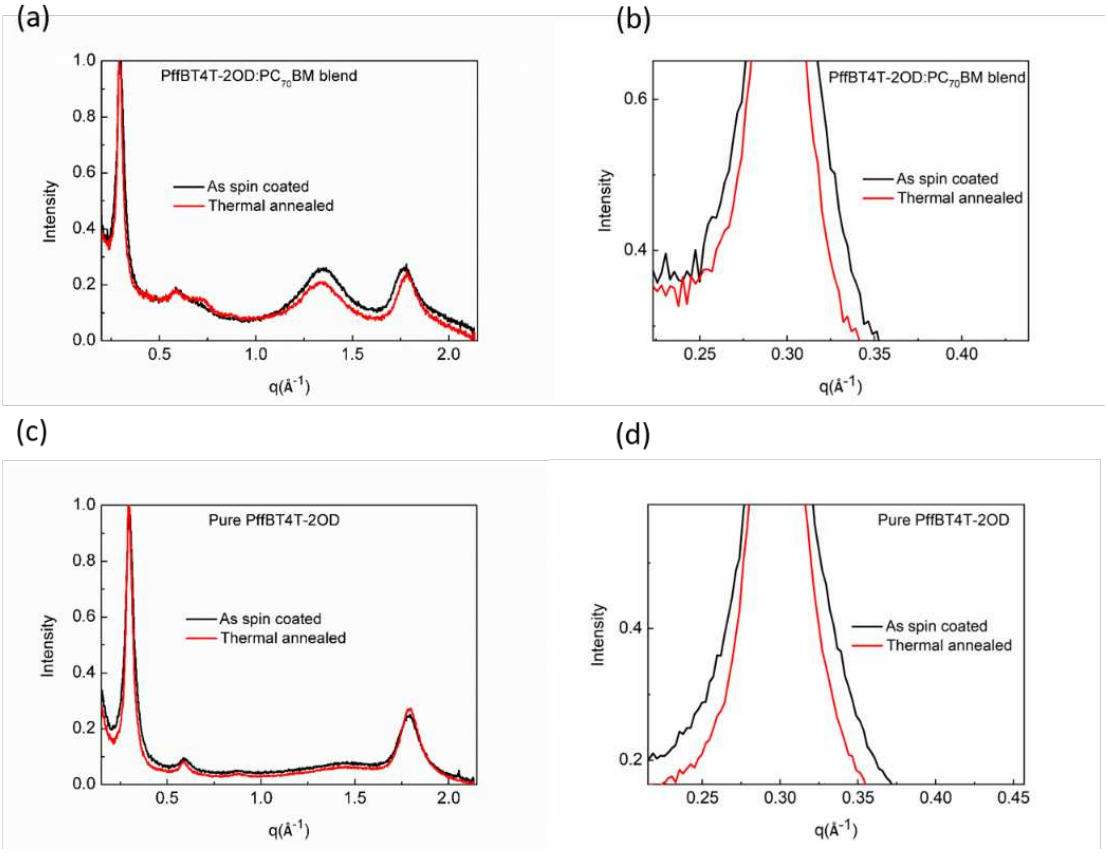

Figure 2. GIWAXS profiles for as-spin coated and thermally annealed PffBT4T-2OD: $PC_{71}BM$ blends (top) neat PffBT4T-2OD films (bottom). The GIWAXS data has been normalized to the (100) peak of PffBT4T-2OD at q=0.30 $Å^{-1}$. The graphs on the right show an expanded view of the (100) diffraction peaks.

Table 2. Determination of PffBT4T-2OD crystallite size.

| Samples | (100) peak position (2θ) (degree) | FWHM of (100) peak (radians) | Crystallite size (nm) |
|---|---|---|---|
| Pure PffBT4T-2OD (As-spin coated) | 3.6523 | 0.01437 | 8.8 |
| Pure PffBT4T-2OD (Thermally annealed) | 3.6526 | 0.00838 | 15.1 |
| PffBT4T-2OD:$PC_{71}BM$ (As-spin coated) | 3.6421 | 0.00958 | 13.2 |
| PffBT4T-2OD:$PC_{71}BM$ (Thermally annealed) | 3.6147 | 0.00712 | 17.8 |

### *3.4 Effect of thermal annealing on exciton diffusion*

We used two methods to measure exciton diffusion in PffBT4T-2OD: surface quenching of fluorescence and exciton-exciton annihilation. For the first method the

fluorescence decays were measured in films deposited on the cross-linked fullerene derivative and compared with decays measured on non-quenching fused silica substrate. These measurements were performed at low excitation density where exciton-exciton annihilations can be neglected. In that case the dynamics of exciton density $N$ can be described by the diffusion equation: [28-29]

$$\frac{\partial N}{\partial t} = D\frac{\partial^2 N}{\partial x^2} - kN - k_F N + G(x) \qquad (2)$$

where $k_F$ is the quenching rate due to Förster resonance energy transfer (FRET) to the quencher, $G(x)$ is the exciton generation rate as a function of position, $D$ is exciton diffusion coefficient and $k$ is the natural decay rate of excitons.

To obtain the diffusion coefficient, we made several assumptions to solve the diffusion equation: Exciton generation is instantaneous as our excitation light pulse is short. No FRET is considered as there is no spectral overlap due to the absorption of PCBSD being at much shorter wavelength than the emission of PffBT4T-2OD.[30] We assume no quenching occurs at the top surface, which gave the boundary condition of $\partial N/\partial x = 0$ at $x=d$, where $d$ is the thickness of the polymer film. At the PffBT4T-2OD/ PCBSD interface, we assume all excitons are quenched giving the second boundary condition of $N = 0$ at $x=0$.

The diffusion equation can be solved numerically. By fitting the fluorescence decay of the PffBT4T-2OD films on top of PCBSD and comparing with the natural decay on fused silica substrates, the exciton diffusion coefficient can be obtained. The experimental and simulated results for three sets of samples are illustrated in **Figure 3** with a diffusion coefficient extracted from fitting. The results show that the average diffusion coefficient increased from 0.8 x $10^{-3}$ to 2.4 x $10^{-3}$ $cm^2/s$ upon thermal annealing.

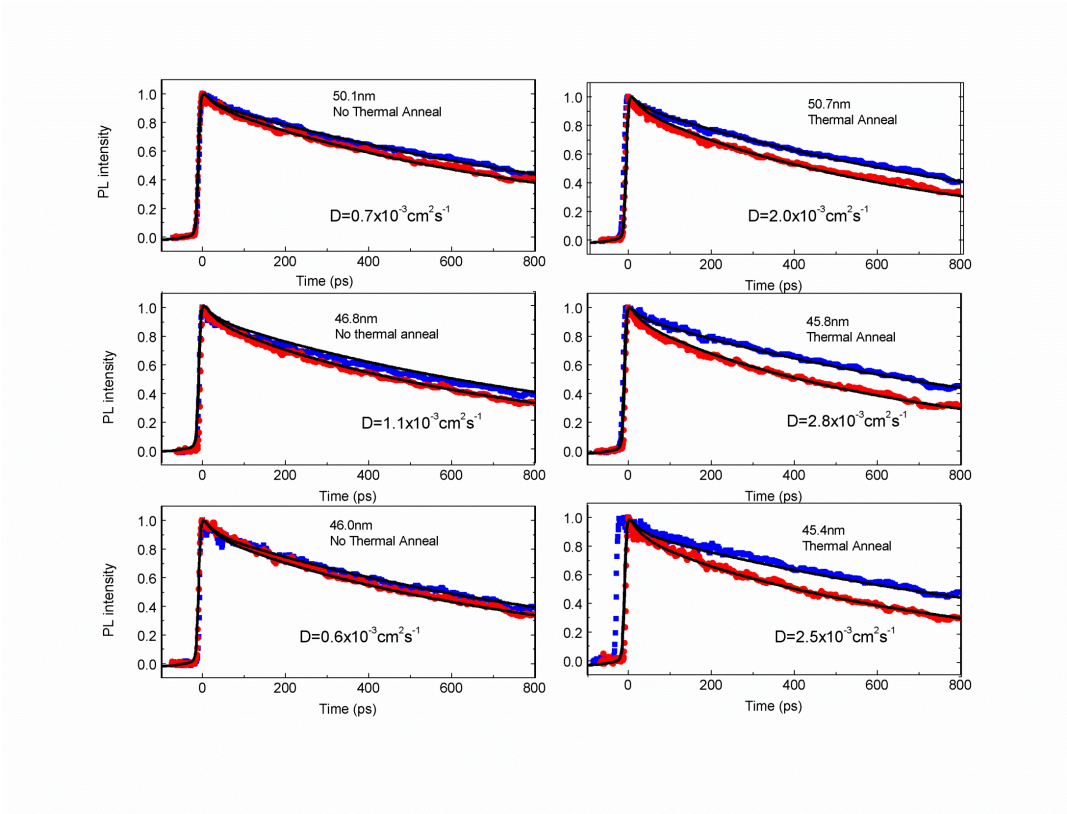


Figure 3. Photoluminescence decays for three sets of PffBT4T-2OD films on fused silica and PCBSD substrates. (excitation wavelength was 515 nm) Fits to the data with the diffusion equation are represented by solid lines.

The surface quenching method measures exciton diffusion in the direction perpendicular to the film surface, however, in BHJ the shortest distance to the electron acceptor could be in any direction. To characterize exciton diffusion in the bulk of the film we used exciton-exciton annihilation measurements (detail given in SI) by measuring time-resolved PL as a function of initial excitation density (Figure 4). Figure 4 shows that fluorescence decays became faster with higher initial exciton populations due to exciton-exciton annihilation.

We fitted the fluorescence decays using Equation (S2) to obtain the annihilation rate constant $\gamma(t)$ which is shown in Figure 4 (c). It can be seen that the annihilation rate constant increased significantly after thermal annealing. The exciton diffusion coefficients (D) determined from the annihilation rate constant are 1.0 x $10^{-3}$ and 3.0 x $10^{-3}$ $cm^2/s$ for as spin-coated and thermally annealed films respectively. We used a value of 2.1 nm for the annihilation radius $R_a$ which is the $d_{100}$ spacing value determined from X-ray data. These values of D are similar to the values obtained using surface quenching which imply that

exciton diffusion is isotropic in PffBT4T-2OD. More discussion can be found in SI. We calculated the 1-dimensional and 3-dimensional exciton diffusion length i. e. $L_D = \sqrt{2D\tau}$ and $L_{3D} = \sqrt{6D\tau}$ using the lifetime value determined from the florescence decay in absence of annihilation (values are indicated in Figure 4).

We summarize the exciton diffusion results obtained from the two different methods in **Table 3**. It can be seen, from both measurements, the exciton diffusion coefficient increased by a factor of 3 upon thermal annealing. As the lifetime did not show significant decrease (being ~1160 and ~1090 ps for as spin-coated and thermally annealed films respectively), the corresponding 1-dimensional exciton diffusion length increased from ~14 nm to ~24 nm and 3-dimensional exciton diffusion length from ~ 25 nm to ~ 42 nm.

Table 3. Exciton diffusion properties determined by two different methods.

| Methods | Surface quenching $D(10^{-3}cm^2/s)$ | Exciton-Exciton annihilation $D(10^{-3}cm^2/s)$ | $L_{1D}$ (nm) | $L_{3D}$ (nm) |
|---|---|---|---|---|
| As spin coated film | 0.8 | 1.0 | 14.4 | 24.9 |
| Thermally annealed film | 2.4 | 3.0 | 24.1 | 41.7 |

*$L_D$ is calculated according to $L_D = \sqrt{2D\tau}$ and $L_{3D} = \sqrt{6D\tau}$, $\tau$ is the time for the fluorescence decay to 1/e of its initial value in absence of annihilation.

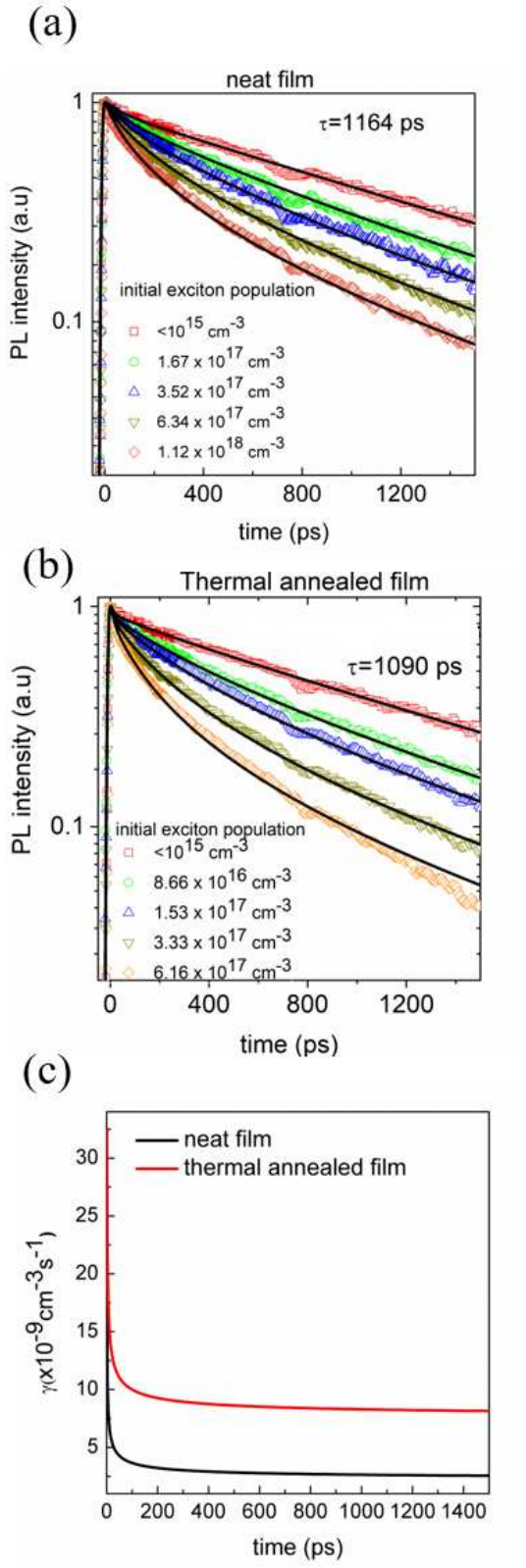


Figure 4. Time-resolved photoluminescence in (a) as-spin coated and (b) thermally annealed films with different initial exciton populations. (c) Annihilation rate constant (γ) in the as-spin coated and thermally annealed films extracted by fitting the time-resolved PL data with equation S2.

## 4. Discussion

We begin by considering the substantial improvement OPV device performance in thermally annealed films and investigate what factors influence this enhancement. From grazing incidence X-ray scattering, we find that the crystallite size increases by 40% upon thermal annealing (i.e. from 13 nm to 18 nm). A larger crystal domain size is usually favourable for higher $V_{oc}$ and FF as there is less recombination. In addition, charge transport and extraction are usually more efficient, with bigger domain sizes leading to an improvement in $J_{sc}$. To investigate charge transport, we fabricated hole only devices with the structure of ITO/PEDOT:PSS/PffBT4T-2OD:$PC_{71}BM$/$MoO_3$/Ag to characterize the hole mobility using SCLC theory [31]. We found a hole mobility of $6.5 \times 10^{-4}$ $V^{-1}$ $s^{-1}$ for as-spin coated and $1.9 \times 10^{-3}$ $cm^2$ $V^{-1}$ $s^{-1}$ for thermally annealed films (See **Figure S3**) The results show that higher crystallinity and larger domain size do indeed result in improved hole mobility which in turn favours better charge extraction. However, with the crystallite domain size exceeding the typical exciton diffusion length of most conjugated polymers, exciton dissociation might be expected to be less efficient, giving lower $J_{sc}$. However, as figure 1(d) shows this is not observed. The high short circuit current is maintained in spite of large domains. this is because the thermal annealing increased the exciton diffusion length to be similar to the crystallite size. The enhanced exciton diffusion length enables efficient exciton dissociation; whilst the larger domains facilitate charge extraction and reduce charge recombination, leading to improved device performance.

We performed an additional measurement of the domain size of the donor by measuring the time-resolved PL of the PffBT4T-2OD:$PC_{71}BM$ blends. The results are shown in Figure 5 which also shows the PL decays of pure PffBT4T-2OD with and without thermal annealing. Compared to pure films, blends show faster PL decay due to exciton dissociation at the interface between donor and acceptor. Among the blends, thermally annealed shows slower decay indication larger crystallite size (domains).

We extracted the size of the PffBT4T-2OD domains in the blend using an approach similar to Hedley et al[32] and Jagadamma et al[33] by considering that PL quenching of the donor in the blend is mediated by exciton diffusion. We assume that the exciton diffuses inside the sphere of the donor (which is surrounded by a $PC_{71}BM$ matrix) by a random walk and is then

quenched at the surface of the sphere. Then the number of excitons *N(t)* on donor molecules is expected to decay with time as follows

$$N(t) = \frac{6}{\pi^2}\sum_{m=1}^{\infty}\frac{1}{m^2}\exp\left(\frac{D\pi^2 m^2 t}{r^2}\right) \qquad (3)$$

where $D$ is the exciton diffusion coefficient and $r$ is the radius of sphere. We used the experimentally measured $D$ = 1.0 x $10^{-3}$ $cm^2/s$ for unannealed film and $D$ = 3.0 x $10^{-3}$ $cm^2/s$ for thermally annealed film.

For fitting, we multiplied equation 2 with the fluorescence intensity of pure PffBT4T-2OD film and then used it to fit the PL decay of the blends (shown in Figure 5). The time-resolved PL measurements suggest that the domain size of PffBT4T-2OD increases from ~12 nm to ~29 nm upon thermal annealing. The general trend of a larger domain size after thermal annealing is the same as for X-ray, but the results differ quantitatively. This could be because of some of the assumptions made in the analysis of the PL such as assuming the donor is spherical in shape, and assuming donor and acceptor phases are entirely separate.

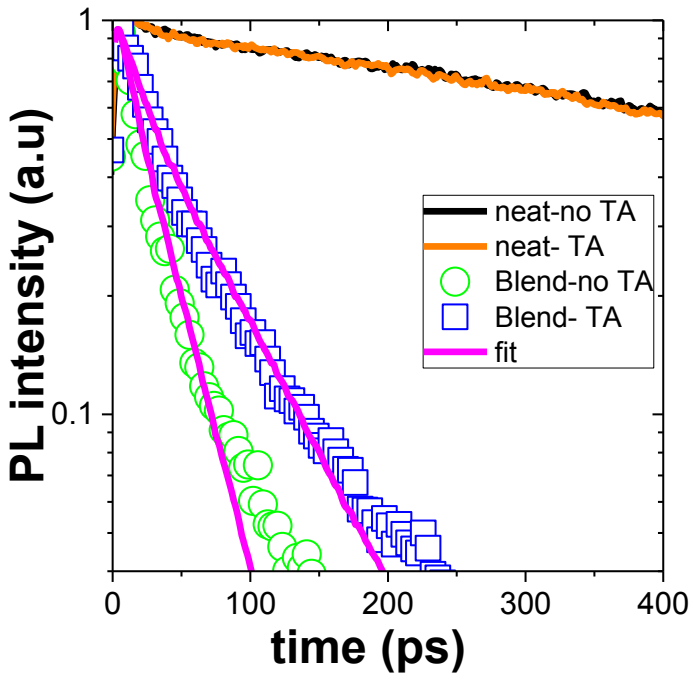


Figure 5. Time-resolved PL quenching of as spin-coated PffBT4T-2OD: $PC_{71}BM$ blend before and after thermal annealing and PL decay of neat PffBT4T-2OD films. TA denotes thermally annealed. Solid red lines are fits to the data using Equation 3.

## 5. Conclusion

In conclusion, we investigated the effect of thermal annealing on crystallite size, exciton diffusion and charge harvesting in PffBT4T-2OD:$PC_{71}BM$ BHJ solar cells. It was found that thermal annealing can significantly increase the crystallite size of PffBT4T-2OD to be much greater than the typical exciton diffusion length for conjugated polymers. However, as the exciton diffusion length was also increased from ~14 to ~24 nm, exciton harvesting is still efficient even in thermally annealed films with large donor crystallite size. The large domains improve the charge extraction efficiency and reduce the charge recombination problem in the devices. Hence our results show that thermal annealing increases both domain size and exciton diffusion length which then lead to an enhancement in the device performance.

## ASSOCIATED CONTENT

Supporting Information is available free of charge via the Internet at http://pubs.acs.org.

## AUTHOR INFORMATION


### Corresponding Author

* Email: idws@st-andrews.ac.uk (I.D.W.S)


### Author Contributions

The manuscript was written through contributions of all authors.
‡Y.Z and M.T.S contributed equally.

### Notes

The authors declare no competing financial interest.


### Acknowledgement

We thank the European Research Council for financial support (EXCITON grant 321305).


## References


ADDIN EN.REFLIST 1. Dou, L.; You, J.; Hong, Z.; Xu, Z.; Li, G.; Street, R. A.; Yang, Y., 25th Anniversary Article: A Decade of Organic/Polymeric Photovoltaic Research. *Adv Mater* **2013,** *25* (46), 6642-6671.

2. Brabec, C. J.; Gowrisanker, S.; Halls, J. J. M.; Laird, D.; Jia, S. J.; Williams, S. P., Polymer-Fullerene Bulk-Heterojunction Solar Cells. *Adv Mater* **2010,** *22* (34), 3839-3856.

3. Yanbo, W.; Yamin, Z.; Nailiang, Q.; Huanran, F.; Huanhuan, G.; Bin, K.; Yanfeng, M.; Chenxi, L.; Xiangjian, W.; Yongsheng, C., A Halogenation Strategy for over 12% Efficiency Nonfullerene Organic Solar Cells. *Adv Energy Mater 0* (0), 1702870.
4. Cheng, P.; Li, G.; Zhan, X.; Yang, Y., Next-generation organic photovoltaics based on non-fullerene acceptors. *Nat Photonics* **2018,** *12* (3), 131-142.
5. Li, S.; Ye, L.; Zhao, W.; Zhang, S.; Mukherjee, S.; Ade, H.; Hou, J., Energy□Level Modulation of Small□Molecule Electron Acceptors to Achieve over 12% Efficiency in Polymer Solar Cells. *Adv Mater* **2016,** *28* (42), 9423-9429.
6. Wenchao, Z.; Sunsun, L.; Shaoqing, Z.; Xiaoyu, L.; Jianhui, H., Ternary Polymer Solar Cells based on Two Acceptors and One Donor for Achieving 12.2% Efficiency. *Adv Mater* **2017,** *29* (2), 1604059.
7. Kirchartz, T.; Taretto, K.; Rau, U., Efficiency Limits of Organic Bulk Heterojunction Solar Cells. *The Journal of Physical Chemistry C* **2009,** *113* (41), 17958-17966.
8. Green, M. A.; Bremner, S. P., Energy conversion approaches and materials for high-efficiency photovoltaics. *Nat Mater* **2016,** *16*, 23.
9. Li, G.; Zhu, R.; Yang, Y., Polymer solar cells. *Nat Photonics* **2012,** *6* (3), 153-161.
10. Blom, P. W.; Mihailetchi, V. D.; Koster, L. J. A.; Markov, D. E., Device physics of polymer: fullerene bulk heterojunction solar cells. *Adv Mater* **2007,** *19* (12), 1551-1566.
11. Barford, W.; Tozer, O. R., Theory of exciton transfer and diffusion in conjugated polymers. *The Journal of Chemical Physics* **2014,** *141* (16), 164103.
12. Ward, A. J.; Ruseckas, A.; Samuel, I. D., A Shift from Diffusion Assisted to Energy Transfer Controlled Fluorescence Quenching in Polymer–Fullerene Photovoltaic Blends. *The Journal of Physical Chemistry C* **2012,** *116* (45), 23931-23937.
13. Hedley, G. J.; Ruseckas, A.; Samuel, I. D., Light harvesting for organic photovoltaics. *Chem. Rev.* **2016,** *117* (2), 796-837.
14. Sajjad, M. T.; Ward, A. J.; Ruseckas, A.; Bansal, A. K.; Allard, S.; Scherf, U.; Samuel, I. D., Tuning the Exciton Diffusion Coefficient of Polyfluorene Based Semiconducting Polymers. *physica status solidi (RRL)–Rapid Research Letters*, 1800500.
15. Mikhnenko, O. V.; Blom, P. W. M.; Nguyen, T.-Q., Exciton diffusion in organic semiconductors. *Energy & Environmental Science* **2015,** *8* (7), 1867-1888.
16. Markov, D. E.; Blom, P. W. M., Anisotropy of exciton migration in poly($p$-phenylene vinylene). *Phys Rev B* **2006,** *74* (8), 085206.
17. Shaw Paul, E.; Ruseckas, A.; Samuel Ifor, D. W., Exciton Diffusion Measurements in Poly(3□hexylthiophene). *Adv Mater* **2008,** *20* (18), 3516-3520.
18. Stevens, M. A.; Silva, C.; Russell, D. M.; Friend, R. H., Exciton dissociation mechanisms in the polymeric semiconductors poly(9,9-dioctylfluorene) and poly(9,9-dioctylfluorene-co-benzothiadiazole). *Phys Rev B* **2001,** *63* (16), 165213.
19. Lewis, A. J.; Ruseckas, A.; Gaudin, O. P. M.; Webster, G. R.; Burn, P. L.; Samuel, I. D. W., Singlet exciton diffusion in MEH-PPV films studied by exciton–exciton annihilation. *Org Electron* **2006,** *7* (6), 452-456.
20. Lunt, R. R.; Giebink, N. C.; Belak, A. A.; Benziger, J. B.; Forrest, S. R., Exciton diffusion lengths of organic semiconductor thin films measured by spectrally resolved photoluminescence quenching. *J Appl Phys* **2009,** *105* (5), 053711.
21. Mullenbach, T. K.; Curtin, I. J.; Zhang, T.; Holmes, R. J., Probing dark exciton diffusion using photovoltage. *Nature communications* **2017,** *8*, 14215.
22. Sajjad, M. T.; Ward, A. J.; Kästner, C.; Ruseckas, A.; Hoppe, H.; Samuel, I. D. W., Controlling Exciton Diffusion and Fullerene Distribution in Photovoltaic Blends by Side Chain Modification. *The Journal of Physical Chemistry Letters* **2015,** *6* (15), 3054-3060.

23. Long, Y.; Hedley, G. J.; Ruseckas, A.; Chowdhury, M.; Roland, T.; Serrano, L. A.; Cooke, G.; Samuel, I. D. W., Effect of Annealing on Exciton Diffusion in a High Performance Small Molecule Organic Photovoltaic Material. *Acs Appl Mater Inter* **2017,** *9* (17), 14945-14952.
24. Liu, Y.; Zhao, J.; Li, Z.; Mu, C.; Ma, W.; Hu, H.; Jiang, K.; Lin, H.; Ade, H.; Yan, H., Aggregation and morphology control enables multiple cases of high-efficiency polymer solar cells. *Nat Commun* **2014,** *5*.
25. Ma, W.; Yang, G.; Jiang, K.; Carpenter, J. H.; Wu, Y.; Meng, X.; McAfee, T.; Zhao, J.; Zhu, C.; Wang, C.; Ade, H.; Yan, H., Influence of Processing Parameters and Molecular Weight on the Morphology and Properties of High-Performance PffBT4T-2OD:PC71BM Organic Solar Cells. *Adv Energy Mater* **2015,** *5* (23), n/a-n/a.
26. Zhang, Y.; Parnell, A. J.; Pontecchiani, F.; Cooper, J. F. K.; Thompson, R. L.; Jones, R. A. L.; King, S. M.; Lidzey, D. G.; Bernardo, G., Understanding and controlling morphology evolution via DIO plasticization in PffBT4T-2OD/PC71BM devices. *Sci Rep-Uk* **2017,** *7*, 44269.
27. Sajjad, M. T.; Blaszczyk, O.; Jagadamma, L. K.; Roland, T. J.; Chowdhury, M.; Ruseckas, A.; Samuel, I. D., Engineered exciton diffusion length enhances device efficiency in small molecule photovoltaics. *Journal of Materials Chemistry A* **2018,** *6* (20), 9445-9450.
28. Scully, S. R.; McGehee, M. D., Effects of optical interference and energy transfer on exciton diffusion length measurements in organic semiconductors. *J Appl Phys* **2006,** *100* (3), 034907.
29. Ward, A. J.; Ruseckas, A.; Samuel, I. D. W., A Shift from Diffusion Assisted to Energy Transfer Controlled Fluorescence Quenching in Polymer–Fullerene Photovoltaic Blends. *The Journal of Physical Chemistry C* **2012,** *116* (45), 23931-23937.
30. Hsieh, C.-H.; Cheng, Y.-J.; Li, P.-J.; Chen, C.-H.; Dubosc, M.; Liang, R.-M.; Hsu, C.-S., Highly Efficient and Stable Inverted Polymer Solar Cells Integrated with a Cross-Linked Fullerene Material as an Interlayer. *J Am Chem Soc* **2010,** *132* (13), 4887-4893.
31. Murgatroyd, P. N., Theory of space-charge-limited current enhanced by Frenkel effect. *Journal of Physics D: Applied Physics* **1970,** *3* (2), 151.
32. Hedley, G. J.; Ward, A. J.; Alekseev, A.; Howells, C. T.; Martins, E. R.; Serrano, L. A.; Cooke, G.; Ruseckas, A.; Samuel, I. D., Determining the optimum morphology in high-performance polymer-fullerene organic photovoltaic cells. *Nature communications* **2013,** *4*.
33. Jagadamma, L. K.; Sajjad, M. T.; Savikhin, V.; Toney, M. F.; Samuel, I. D., Correlating photovoltaic properties of a PTB7-Th: PC 71 BM blend to photophysics and microstructure as a function of thermal annealing. *Journal of Materials Chemistry A* **2017,** *5* (28), 14646-14657.